

Photoelectrochemical Properties of RuS₂-Coated TiO₂ Electrodes

Muthupandian Ashokkumar,[#] Akihiko Kudo,^{##} and Tadayoshi Sakata^{*}

Department of Electronic Chemistry, Interdisciplinary Graduate School of Science and Engineering,
Tokyo Institute of Technology, 4259 Nagatsuta, Midori-ku, Yokohama 226

(Received December 22, 1994)

Photoelectrochemical studies of RuS₂-coated TiO₂ electrodes showed semiconductor sensitization by RuS₂ fine particles on TiO₂. RuS₂ particles of ca. 100 nm size were observed from a scanning electron micrograph of the RuS₂/TiO₂ electrode surface. RuS₂-coated TiO₂ electrodes showed continuous wide absorption in the visible spectral region. Photoelectrochemical measurements of several RuS₂/TiO₂ electrodes, prepared under different conditions, were carried out. The electron-transfer efficiency from RuS₂ to TiO₂ was affected by the number of RuS₂ colloid coatings and the preparation temperature of the RuS₂ colloids. A schematic study was carried out on the effect of a heat treatment in order to find the optimum temperature for the maximum sensitization efficiency. A comparison of the absorption and action spectra of the RuS₂/TiO₂ electrode showed that only small RuS₂ particles with a critical size distribution could transfer the photo-generated electrons to TiO₂. A band-gap value of ca. 2.8 eV was evaluated (from the photocurrent action spectrum) for the RuS₂ particles with high sensitization efficiency. A scheme which shows the energy diagram for RuS₂ fine particles has been proposed by considering the flat-band potential values derived from the photocurrent onset potentials and the above-mentioned band-gap value.

The photoelectrochemical conversion of light energy into electrical energy and other utilizable forms using semiconductor electrodes has been extensively investigated during the past few decades.^{1–5)} Chalcogenides of transition metal ions were found to be efficient materials for this purpose,^{6–10)} due to their wide absorption in the visible spectral region. RuS₂ was proved to be highly resistant to photocorrosion.¹¹⁾ Other advantages of this material are its narrow band-gap (1.3–1.85 eV),^{12–15)} good photoelectrochemical efficiency and stability in H₂ and O₂ evolution experiments.^{13,15,16)} The photoelectrochemical properties of poly- and single-crystalline RuS₂ electrodes have been extensively investigated by Tributsch and co-workers.^{11,13,15–19)}

Photosensitization by adsorbed organic dye, inorganic complex molecules^{20–24)} and narrow band-gap semiconductors^{25–29)} was found to be a good technique to increase the photoelectrochemical efficiencies of wide band-gap semiconductors. In the former case, after dye molecules are excited by low-energy photons, electrons are injected into the conduction band of the host semiconductor from these excited states. In the latter case, photo-generated conduction-band electrons of narrow band-gap semiconductors are transferred to the conduc-

tion bands of wide band-gap semiconductors; this phenomenon was named “semiconductor sensitization”.²⁷⁾

We have recently succeeded to prepare RuS₂ nanocrystallites,³⁰⁾ and have reported some preliminary experimental results concerning the application of this material for semiconductor sensitization experiments.³¹⁾ In this article we discuss our systematic investigations concerning the effect of the number of RuS₂ coatings as well as the preparation temperature and heat-treatment temperature of RuS₂ colloids with regard to the semiconductor-sensitization efficiency of RuS₂ over TiO₂.

Experimental

Details concerning the preparation method of RuS₂ colloids and their characterization using different techniques have been reported elsewhere.³⁰⁾ A brief description of the preparation method is given here: RuS₂ colloids were prepared using a 0.1–0.2 M RuCl₃ (1 M=1 mol dm⁻³) (99.9%; Wako Pure Chem. Ind. Ltd.) solution in sulfolane, and bubbling H₂S for long time with constant stirring at different temperatures. The following method was used to make RuS₂-coated TiO₂ electrodes: Pellets of ca. 2 mm thickness and ca. 20 mm diameter were made using commercially available TiO₂ powder (99.99%; Rutile, Wako Pure Chem. Ind. Ltd.). These pellets were first sintered at 1200 °C for 10 h in air, and then reduced at 600 °C under an H₂ atmosphere for 3 h. On one side of these pellets, an RuS₂ colloidal solution was coated using a K-359SD-270 Spinner (Kyowa Riken), and dried at 150 °C under a vacuum. The resulting RuS₂-coated TiO₂ pellets were heat-treated under

[#]JSPS fellow from Department of Energy, University of Madras, India.

^{##}Present address; Department of Applied Chemistry, Faculty of Science, Science University of Tokyo, 1-3 Kagurazaka, Shinjuku-ku, Tokyo 162.

an argon atmosphere at different temperatures for ca. 3 h in order to increase the stability of the coating and to remove any trace amounts of solvent that might still be adsorbed. Ohmic contacts between an uncoated surface of the pellets and copper wires were made using an In–Ga alloy; the surfaces were covered with an epoxy resin.

The $\text{RuS}_2/\text{TiO}_2$ electrode surface was analyzed with a scanning electron microscope (JEOL JSM-T220). Absorption and diffuse reflection measurements were carried out using a UV-visible spectrophotometer (UV-2100PC, Shimadzu). Photoelectrochemical measurements were carried out using a cell comprising the semiconductor working electrode, a Pt counter electrode and an Ag/AgCl reference electrode. The electrolyte concentrations are given in the respective figure captions. The short-circuit action spectra of the photoanodes were recorded by measuring the photocurrents with an amplifier attached to the FluoroMax, whose monochromatic light source (150 W Xe lamp) was used for irradiation. The electrode potential was controlled by a potentiostat (Hokuto Denko, HA-3001), and was swept by a function generator (Hokuto Denko, HB-107). Photocurrent–voltage measurements were also made using the same experimental arrangement with a 500 W Xe-lamp (Ushio Electric Inc.) for irradiation of the electrode surfaces.

Results and Discussion

Figure 1 shows a scanning electron micrograph of an $\text{RuS}_2/\text{TiO}_2$ electrode surface. Submicron-sized (ca. 100 nm) RuS_2 particles on the surface of TiO_2 are clearly visible in Fig. 1. A detailed investigation of the characterization of RuS_2 nanocrystallites has already been reported.³⁰⁾ XRD measurements showed the existence of RuS_2 with a fine crystal size (<50 nm). Although they were not RuS_2 on TiO_2 , a similar argument could be applied to the present system. The RuS_2 particles observed by SEM may comprise smaller particles, or small particles invisible to SEM might exist on the TiO_2 surface. Figure 2 shows the absorption spectra of $\text{RuS}_2/\text{TiO}_2$ and TiO_2 electrodes, derived from diffuse reflection measurements. As can be seen in this figure,

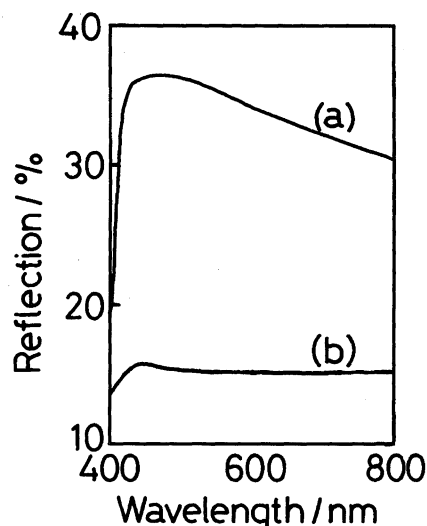


Fig. 2. Diffuse reflection spectra of (a) TiO_2 and (b) $\text{RuS}_2/\text{TiO}_2$ (4 coatings) electrodes.

the $\text{RuS}_2/\text{TiO}_2$ electrode showed continuous absorption in the visible region of the spectrum. One can understand that the increased absorption in the visible region is due to RuS_2 . This observation also agrees with the absorption spectra of RuS_2 colloids, thin film on a glass substrate and RuS_2 powders.^{30,31)}

The transfer of photo-generated electrons from RuS_2 to TiO_2 was confirmed from the photocurrent action spectrum of an $\text{RuS}_2/\text{TiO}_2$ electrode (Fig. 3). As can be seen in this figure, the photocurrent action spectrum of $\text{RuS}_2/\text{TiO}_2$ is considerably red-shifted compared to that of TiO_2 , showing the semiconductor sensitization effect due to RuS_2 . The difference between the action spectra of $\text{RuS}_2/\text{TiO}_2$ and TiO_2 electrodes is also shown in the insert of Fig. 3. For clarity, the action spectrum recorded by chopping the incident light is also given in Fig. 3 in order to show the response of this electrode up to 550–600 nm. The photocurrent action spectrum of the $\text{RuS}_2/\text{TiO}_2$ electrode shown in Fig. 3 is represen-

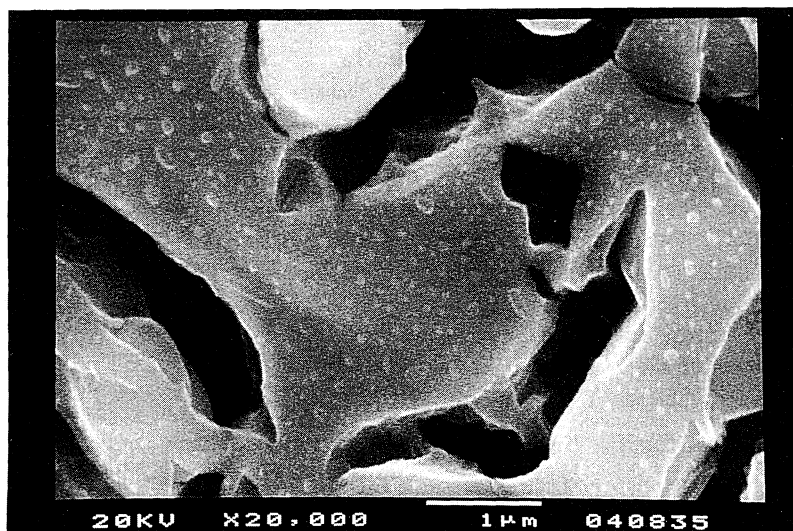


Fig. 1. Scanning electron micrograph of a $\text{RuS}_2/\text{TiO}_2$ electrode surface (4 coatings).

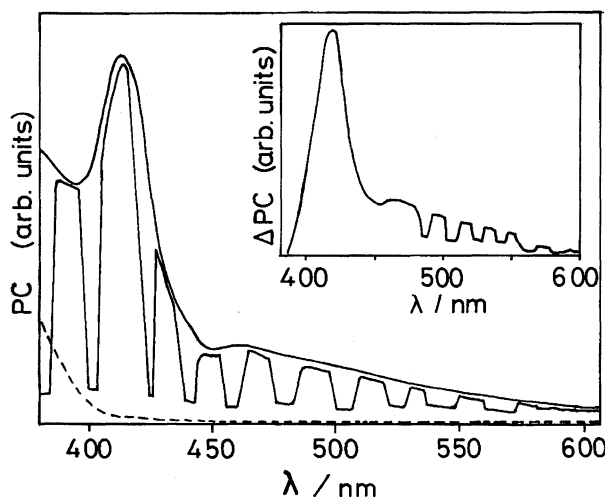


Fig. 3. Photocurrent action spectra of a $\text{RuS}_2/\text{TiO}_2$ electrode (4 coatings; electrolyte: 0.5 M K_2SO_4): to show the photoeffect until ca. 600 nm, photocurrent action spectrum by chopping the incident light is also shown; the photocurrent action spectrum of TiO_2 is shown in the dotted line; the inset is the difference between the photocurrent action spectra of $\text{RuS}_2/\text{TiO}_2$ and $\text{TiO}_2^{31)}$ electrodes; λ =wavelength; PC=photocurrent.

tative. A similar behavior was also observed with all $\text{RuS}_2/\text{TiO}_2$ electrodes with different efficiencies. However, it must be mentioned that the photocurrent onset wavelength for these electrodes was blue-shifted compared to that (ca. 670 nm) of poly- and single crystalline RuS_2 electrodes,¹³⁾ probably due to a size-quantization effect. The submicron-sized (100 nm) RuS_2 particles appearing in Fig. 1 may not satisfy the observed shift in the photocurrent onset wavelength, compared to that of the bulk material, suggesting still smaller RuS_2 particles on the TiO_2 electrode surface, which were responsible for the size-quantization effect. XRD analyses support this argument, as mentioned above.

A typical current–voltage curve for an $\text{RuS}_2/\text{TiO}_2$ electrode is given in Fig. 4. The amount of dark current in the cathodic region was very high (Fig. 4a), and a measurement of the photocurrent in this region was difficult. The photocurrent appeared at approximately -0.8 V (vs. Ag/AgCl). In the anodic region (Fig. 4b) the photocurrent gradually increased along with an increase in the applied voltage, and approached a saturation limit at approximately $+2.0$ V (vs. Ag/AgCl). The flat-band potentials (E_{fb}) of the $\text{RuS}_2/\text{TiO}_2$ electrodes were assumed to be approximately the same as those of the photocurrent onset potentials. Since the current was not very large near to the flat-band potential, the effect of a change in the pH on the potential shift is thought to be negligible. The band-gap (E_g) value of RuS_2 particles which could inject electrons to TiO_2 electrodes was determined to be ca. 2.8 eV from a plot of $h\nu$ vs. $(\text{PC} \times h\nu)^{1/2}$ by extrapolating the linear part

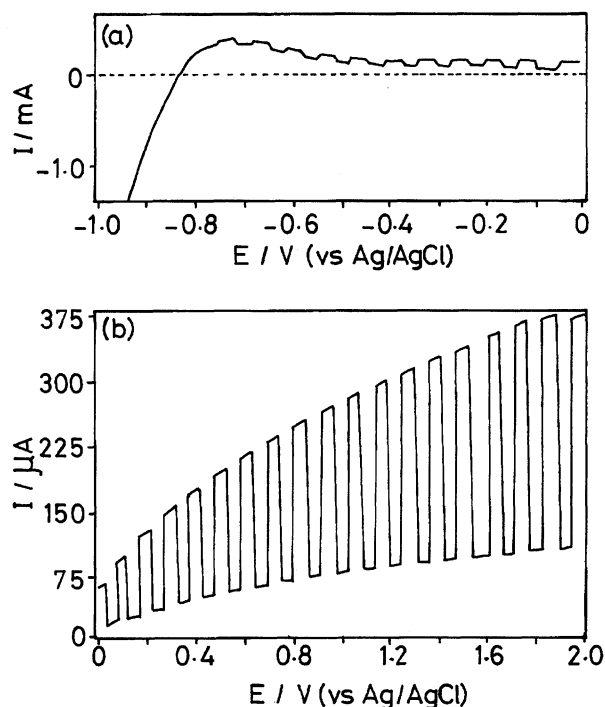


Fig. 4. Photocurrent–voltage curve for a typical $\text{RuS}_2/\text{TiO}_2$ electrode in 0.5 M K_2SO_4 ; (a) cathodic region; (b) anodic region.

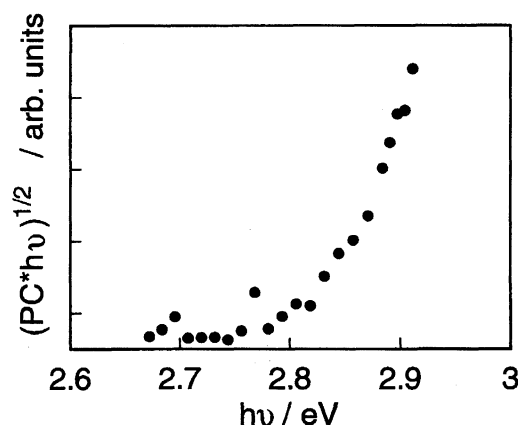


Fig. 5. Plot for band-gap energy determination.

(Fig. 5). A schematic representation of the energetic of RuS_2 and TiO_2 is proposed in Fig. 6, by considering the E_{fb} and E_g values, and the energy levels of TiO_2 .²⁹⁾ It can be understood from this scheme that the conduction band of RuS_2 is located at a more negative potential than that of TiO_2 , and that the transfer of photo-generated electrons from RuS_2 to TiO_2 is energetically well favored. It should also be understood that the band-gap energy determined from Fig. 5 is the smallest one with which RuS_2 particles can inject electrons to TiO_2 . A band-gap energy determination based on the absorption spectrum would result in a comparatively smaller value and the band gap energy would be different from those proposed in the scheme, due to the larger particles. Since we are concerned with the semiconductor-

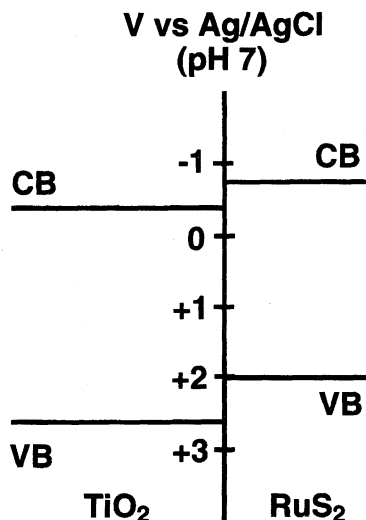


Fig. 6. Schematic representation of the energetics of RuS₂ and TiO₂.

sensitization efficiency, we used the photocurrent for the band-gap determination instead of the absorption coefficient in Fig. 5. Hence, the band-gap value determined from Fig. 5 and the energetics proposed in the scheme are those proposed for RuS₂ particles with a critical-size distribution showing a better sensitization efficiency.

The photocurrents (I_{ph}) without and with a 420 nm cut-off filter, photovoltages (V_{ph}) and onset potentials (E_{onset}), observed in 0.5 M K₂SO₄ and 1 M H₂SO₄, with RuS₂/TiO₂ electrodes prepared at different conditions, are summarized in Table 1. The amounts of photocurrents did not decrease upon continuous illumination of the electrodes (with filter) for more than 10 h, which reflects the photostability of RuS₂. The general trend observed for the photocurrents and photovoltages with these electrodes was similar in both electrolytes. The photocurrents observed without a 420 nm filter were higher due to the larger number of high-energy photons. Both TiO₂ and RuS₂ must be excited by $\lambda < 420$ nm photons, and the photocurrents observed might reflect the efficiencies of both semiconductors. However, when we compared the magnitudes of these photocurrents with that of TiO₂ alone, some showed decreases in the photocurrents, reflecting the fact that coated-RuS₂ showed a shielding effect on the photocurrent due to TiO₂. However, the photocurrent magnitudes observed for RuS₂-coated TiO₂ electrodes with the 420 nm cut-off filter were considerably higher than that of TiO₂ alone (with some exceptions). Another argument (instead of the shielding effect) could be suggested to explain this observed trend when we consider the effect of the number of coatings of RuS₂ colloids on the photocurrent. For an easy understanding, the effect of the number of coatings on the photocurrent is plotted in Fig. 7. As shown in this figure, compared to TiO₂ alone, a single coating resulted in a decrease in the photocurrent without a filter. This would be due to a shielding effect in

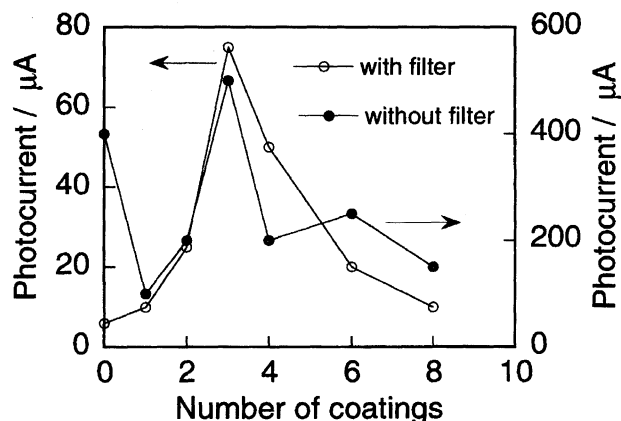


Fig. 7. Effect of the number of coatings on the photocurrent.

which RuS₂ partly blocked the TiO₂ surface, and thus a large contribution to the photocurrent by TiO₂ was suppressed. However, with a 420 nm cut-off filter, an increase in the photocurrent was noticed, even for a single coating. Along with a further increase in the number of coatings, the photocurrent increased, reached a maximum for 3 coatings and decreased for 4–8 coatings. It is worth mentioning that the photocurrent increased ca. 5–7 times (without and with a filter) for 3 coatings, compared to that of a single coating. This leads to a major conclusion that RuS₂ is mainly responsible for the photocurrent observed without (except for a single coating) and with a filter. If we considered shielding effects by RuS₂ over TiO₂, we should have had a decrease in the photocurrent without a filter, since most of the protons would be absorbed by an increased number of RuS₂ particles along with an increase in the number of coatings. However the observed results showed an opposite effect, confirming that RuS₂ is the primary photoactive material in these electrodes, and that TiO₂ has a very low contribution to the photocurrent. The decreased photocurrent observed with an additional increase in the number of coatings might be due to the thickness of the RuS₂ layer, which showed a shielding effect for the photons to reach the inner-most layer of RuS₂, in contact with the TiO₂ surface, that resulted in a small number of electron-hole pair generation in the effective layer of the RuS₂ colloids. The increase in the number of coatings would also have caused a clustering of the colloidal particles where electron-transfer into TiO₂ is less efficient, since the electron-transfer distance becomes longer in the clustered aggregates, and grain boundaries may serve as recombination centers for the photo-generated electron-hole pairs. The instability of the film above 8 coatings could also be explained by the same reason. Clustering would also decrease the contact area between RuS₂ particles and the TiO₂ surface causing the instability. However, the photovoltages observed for these electrodes increased along with the number of coatings (Table 1).

Table 1. Effects of the No. of Coatings, Preparation Temperature and Heat-Treatment on the Semiconductor Sensitization by RuS₂ on TiO₂

$T_{\text{preparation}}$ °C	$T_{\text{heat-treat.}}$ °C	Number of coatings	$I_{\text{ph}}/\mu\text{A}$ (no filter)	$I_{\text{ph}}/\mu\text{A}$ ($\lambda > 420$ nm)	V_{ph}/mV (no filter)	E_{onset} mV
150	400	1	100 (150)	10 (20)	10 (<10)	-850
150	400	2	200 (150)	25 (20)	50 (20)	-870
150	400	3	500 (500)	75 (50)	100 (20)	-850
150	400	4	200 (150)	50 (25)	90 (30)	-820
150	400	6	250 (200)	20 (25)	150 (40)	-710
150	400	8	150 (100)	10 (10)	200 (40)	-690
150	400	10	Not stable			
50	400	3	250 (200)	30 (50)	10 (<10)	-800
100	400	3	500 (400)	50 (50)	100 (50)	-800
200	400	3	400 (400)	60 (50)	150 (50)	-830
200	As-dried	4	20 (50)	<5 (<10)	10 (<10)	-830
200	200	4	100 (100)	30 (25)	100 (30)	-900
200	400	4	250 (200)	50 (50)	100 (40)	-800
200	600	4	50 (100)	10 (<10)	80 (40)	-600

Photocurrents observed at 1.0 V (vs. Ag/AgCl) applied potential; Electrolyte: 0.5 M K₂SO₄; values given within brackets were observed in 1 M H₂SO₄; for TiO₂, 400 μA and <10 μA were observed without and with filter, respectively (in K₂SO₄).

Since the photoactivity of RuS₂ strongly depended upon the preparation conditions,¹⁴⁾ we varied the temperature during the preparation of RuS₂ colloids. Experimental observations (Table 1) showed that the colloids prepared at 50 °C considerably increased the photocurrent with the 420 nm cut-off filter. When the preparation temperature was further increased, the sensitization efficiency increased until 150 °C, and then decreased above this temperature. The photovoltage also increased along with an increase in the preparation temperature. The preparation temperature would affect the crystallinity of RuS₂ colloids and their contact with a TiO₂ substrate, resulting in an improvement in the photocurrent efficiency. The effect of a heat-treatment of the RuS₂-coated TiO₂ pellets on the photocurrent was also investigated; the results are shown in Table 1. Coatings of narrow band-gap semiconductor colloidal particles over wide band-gap semiconductors need a heat-treatment in order to increase the stability of these particles under different photoelectrochemical conditions. In general, a heat-treatment would result in an increase in the crystal size. If the heat-treatment resulted in the growth of these nanocrystallites to larger crystals, that would decrease the contact area between the surfaces of the two semiconductors. This would decrease the electron-transfer efficiency from the sensitizer, which, in turn, would affect the semiconductor sensitization efficiency on wide band-gap semiconductors. The absence of such growth in crystal size in our case, as observed in the photocurrent action spectrum (the size quantization effect, as discussed earlier), is an additional advantage for increasing the sensitization efficiency of RuS₂. The as-dried electrode (without heat-treatment) showed a very low photocurrent, and the film was unstable after a few minutes of photoelectrochemical experiments (Table 1). This

might have been due to the poor contact between the RuS₂ particles and the TiO₂ surface in the absence of a heat-treatment. An energy-dispersive X-ray analysis (EDX) showed that included-solvent molecules for samples without heat-treatment³⁰⁾ could also be responsible for this poor contact. In addition, the XRD investigation³⁰⁾ for RuS₂ nanocrystallites showed that the crystallinity (no change in crystal structure) was increased by a heat treatment. The improvement in the crystallinity due to the heat treatment probably contributed to the increase in the photocurrent efficiency. A maximum photocurrent was observed for an electrode heat-treated at 400 °C, and a further increase in the heat-treatment temperature resulted in a decrease in the photocurrent (Table 1). This might have been due to an increase in the crystal size, which affected the electron-transfer efficiency from RuS₂ to TiO₂. Except for the as-dried electrode, others showed approximately the same photovoltages in both electrolytes.

The photocurrent onset-potential values for all RuS₂-coated TiO₂ electrodes were measured in 0.5 M K₂SO₄, and are given in Table 1. The onset of photocurrents was between ca. -0.9 and -0.6 V (vs. Ag/AgCl), depending on the preparation conditions. For the electrodes prepared with 1–4 coatings, the onset-potentials were approximately the same. For 6 and 8 coatings, values of ca. -0.7 V were observed, showing that E_{fb} (and so the conduction band position) moved ca. +0.1 eV. This might have been due to an increase in the particle size with an increase in the number of coatings. For other electrodes, values of around -0.8 V were observed, except for that prepared at 600 °C, again showing an increase in the particle size. Since the concentration of RuS₂ particles was higher with an increase in the number of coatings, the possibility for growth in the particle size was higher. Also, a higher heat-treatment

temperature would favor the growth of these particles, resulting in a shift of the condition band level towards the positive direction.

Conclusions

The band-gap value of sub-micron RuS_2 particles is wider than that of the bulk material.^{12–15} A size-quantization effect was responsible for this band-gap widening. Better sensitization by RuS_2 particles with a critical-size distribution could be understood from the scheme shown in Fig. 6. For larger RuS_2 particles, the conduction-band level shifted closer to that of TiO_2 , and decreased the electron-transfer efficiency. The discrepancy between the absorption and action spectra of $\text{RuS}_2/\text{TiO}_2$ could also be understood by considering the same argument. The photoelectrochemical properties of $\text{RuS}_2/\text{TiO}_2$ also showed that the sensitization efficiency was also influenced by the number of coatings, preparation and heat-treatment temperatures. Especially, a heat-treatment at 400 °C was indispensable for obtaining a high photocurrent. In most cases, the size-quantization effect was responsible for the difference in the efficiencies between electrodes.

Financial support from the Japan Society for the Promotion of Science (JSPS) is gratefully acknowledged by M.A.

References

- 1) A. J. Nojik, *Ann. Rev. Phys. Chem.*, **29**, 189 (1978).
- 2) M. S. Wrighton, *Acc. Chem. Res.*, **12**, 303 (1979).
- 3) F. Cardon, W. P. Gomes, and W. Dekeyser, "Photo-voltaic and Photoelectrochemical Solar Energy Conversion," NATO ASI Series B, Plenum, New York (1980), p. 69.
- 4) M. Schiavello, "Photoelectrochemistry, Photocatalysis and Photoreactors: Fundamentals and Developments," NATO ASI Series C, D. Reidel Pub. Co., Dordrecht (1985), p. 146.
- 5) C. A. Koval and J. N. Howard, *Chem. Rev.*, **92**, 411 (1992), and other references therein.
- 6) T. Kawai, H. Tributsch, and T. Sakata, *Chem. Phys. Lett.*, **69**, 336 (1980).
- 7) H. Tributsch and O. Gorochov, *Electrochim. Acta*, **27**, 215 (1982).
- 8) H.-M. Kuhne, W. Jaegermann, and H. Tributsch, *Chem. Phys. Lett.*, **112**, 160 (1984).
- 9) A. Ennaoui, S. Fiechter, W. Jaegermann, and H. Tributsch, *J. Electrochem. Soc.*, **133**, 97 (1986).
- 10) T. Sakata, E. Janata, W. Jaegermann, and H. Tributsch, *J. Electrochem. Soc.*, **133**, 339 (1986).
- 11) R. Heindl, R. Parsons, A. M. Redon, H. Tributsch, and J. Vigneron, *Surface Sci.*, **115**, 91 (1982).
- 12) F. Hulliger, *Nature.*, **200**, 1064 (1963).
- 13) H. Ezzaouia, R. Heindl, R. Parsons, and H. Tributsch, *J. Electroanal. Chem.*, **145**, 279 (1983).
- 14) D. H. M. W. Thewissen, E. A. van der Z-Assink, K. Timmer, A. H. A. Tinnemans, and A. Mackor, *J. Chem. Soc., Chem. Commun.*, **1984**, 941.
- 15) H.-M. Kuhne and H. Tributsch, *J. Electroanal. Chem.*, **201**, 263 (1986).
- 16) S. Piazza, H.-M. Kuhne, and H. Tributsch, *J. Electroanal. Chem.*, **196**, 53 (1985).
- 17) R. Guittard, R. Heindl, R. Parsons, A. M. Redon, and H. Tributsch, *J. Electroanal. Chem.*, **111**, 401 (1980).
- 18) H. Ezzaouia, R. Heindl, R. Parsons, and H. Tributsch, *J. Electroanal. Chem.*, **165**, 155 (1984).
- 19) N. A.-. Vante, H. Colell, and H. Tributsch, *J. Phys. Chem.*, **97**, 8261 (1993).
- 20) H. Gerischer and H. Tributsch, *Ber. Bunsenges. Phys. Chem.*, **72**, 437 (1968).
- 21) H. Gerischer and F. Willig, *Top. Curr. Chem.*, **61**, 31 (1976).
- 22) K. Hashimoto, M. Hiramoto, and T. Sakata, *J. Phys. Chem.*, **92**, 4272 (1988).
- 23) T. Sakata, K. Hashimoto, and M. Hiramoto, *J. Phys. Chem.*, **94**, 3040 (1990), and other references therein.
- 24) I. Bedja, S. Hotchandani, and P. V. Kamat, *J. Phys. Chem.*, **98**, 4133 (1994), and other references therein.
- 25) R. Vogel, K. Pohl, and H. Weller, *Chem. Phys. Lett.*, **174**, 241 (1990).
- 26) A. Ennaoui, S. Fiechter, H. Tributsch, M. Giersig, R. Vogel, and H. Weller, *J. Electrochem. Soc.*, **139**, 2514 (1992).
- 27) S. Kohtani, A. Kudo, and T. Sakata, *Chem. Phys. Lett.*, **206**, 166 (1993).
- 28) D. Liu and P. V. Kamat, *J. Phys. Chem.*, **97**, 10769 (1993).
- 29) R. Vogel, P. Hoyer, and H. Weller, *J. Phys. Chem.*, **98**, 3183 (1994).
- 30) M. Ashokkumar, A. Kudo, and T. Sakata, *J. Mater. Sci.*, **30**, 2759 (1995).
- 31) M. Ashokkumar, A. Kudo, N. Saito, and T. Sakata, *Chem. Phys. Lett.*, **299**, 383 (1994).